

Disentanglement as a strong cosmic censor

Hong Zhe Chen

hzchen@ucsb.edu

Department of Physics
Broida Hall
University of California
Santa Barbara, CA 93106-9530, USA

Abstract

If entanglement builds spacetime, then conversely, disentanglement ought to destroy spacetime. From the quantum null energy condition and quantum focusing conjecture, we obtain disentanglement criteria which necessitate infinite energies and strong spacetime singularities. We apply our results to the strong cosmic censorship proposal, where strong singularities at the Cauchy horizons in black holes are desirable. Using our disentanglement criteria and without resorting to any detailed calculations, we provide an exceedingly general and physically transparent discussion of strong cosmic censorship in semiclassical black holes. We argue that strong cosmic censorship is enforced in asymptotically flat and de Sitter black holes by disentanglement and describe how similar disentanglement might be avoided in some anti-de Sitter cases.

Essay written for the Gravity Research Foundation 2024 Awards for Essays on Gravitation. Extra commentary and examples have been added as footnotes and an appendix.

Contents

1	Introduction	1
2	Entanglement at short distances	2
3	The QNEC and the QFC	3
4	Disentanglement and its consequences	4
5	Strong cosmic censorship	6
6	Disentanglement across the Cauchy horizon	7
7	Conclusion	10
A	Energy and entanglement in two-dimensional CFTs	10
A.1	A joining quench example	11
A.2	Stationary black hole backgrounds	14
A.2.1	The geometry and useful coordinates	15
A.2.2	State preparation	17
A.2.3	Energy and entanglement	19

1 Introduction

A motif that appears in the study of quantum information in gravity is the notion that entanglement builds spacetime geometry [1]. Taken literally, the entanglement between naively distant degrees of freedom is recast as geometric wormholes [2]. More abstractly, the identification of black hole interiors with Hawking radiation through entanglement has recently revealed a partial resolution [3, 4] to the infamous information paradox [5, 6]. In this essay, we will explore the converse idea: disentanglement breaks apart spacetime geometry [1, 7].

We will focus particularly on short-distance entanglement in quantum field theories (QFTs) on semiclassical backgrounds, and the consequences of destroying this entanglement. To connect entanglement to energy and its imprint on spacetime geometry, we will appeal to the quantum null energy condition and quantum focusing conjecture [8], which govern QFTs in semiclassical spacetimes. These considerations will motivate disentanglement criteria which unavoidably lead to infinite energies and strong spacetime singularities.

Such singularities are sometimes desirable. In particular, certain black holes contain Cauchy horizons which delimit the unique evolution from initial data or states on an initial time slice. Naively, the breakdown of the theory’s predictive power beyond the Cauchy horizon seems problematic. However, strong cosmic censorship (SCC) postulates that solutions will generically develop singularities at or before the Cauchy horizon and cannot be further

extended [9]. Though classically violated in certain situations, SCC seems to be restored semiclassically by quantum fields [10].

Using our disentanglement criteria, we will provide an exceedingly general argument for SCC that can be narrated by words and pictures alone. Our story cohesively ties together results previously reliant on explicit calculations in specific backgrounds, in particular generalizing and strengthening previous considerations of entanglement in the context of SCC [11]. With this application to SCC, we aim to illustrate the useful sensitivity of spacetime geometry to the destruction of entanglement.

2 Entanglement at short distances

The entanglement of interest to us will be between spatial subregions — let us begin by quantifying this entanglement. In QFT, the state of quantum fields in a spatial subregion R can be formally described by a density matrix ρ_R . For example, if R is a subregion of a full time slice $R \cup \bar{R}$ on which the quantum fields are in a pure state $|\psi\rangle$, then the reduced state $\rho_R = \text{tr}_{\bar{R}} |\psi\rangle \langle\psi|$ on R would be obtained by tracing over the Hilbert space in the complementary subregion \bar{R} . A simple measure of entanglement between R and its complement is then given by the von Neumann entropy,

$$S_R = -\log(\rho_R \log \rho_R) . \quad (1)$$

For our purposes, it will be helpful to isolate the entanglement strictly between two subregions R_1 and R_2 which need not be complementary. The relevant quantity in this regard is the mutual information

$$I_{R_1:R_2} = S_{R_1} + S_{R_2} - S_{R_1 \cup R_2} , \quad (2)$$

which subtracts off the contribution from entanglement with everything outside $R_1 \cup R_2$.

Both the entropy (1) and the mutual information (2) between *adjacent* subregions are positively divergent in QFT, due to the entanglement between degrees of freedom supported arbitrarily close to the entangling surfaces ∂R and $\partial R_1 \cap \partial R_2$. In smooth states, the excitations of these degrees of freedom are exponentially suppressed in energy above the locally Minkowskian vacuum. Nonetheless, there are significant correlations in the quantum fluctuations across the entangling surface, as visible, for example, from a locally Rindler perspective [12, 11].¹ Fortunately, the same short-distance entanglement structure is shared by all smooth states. The divergences in eqs. (1) and (2) can therefore be cancelled by state-independent

¹Locally, one can view null hypersurfaces orthogonal to the entangling surface as Rindler horizons orthogonal to a bifurcation surface in an approximate Minkowski spacetime. The authors of [11] showed that smooth states of free fields have localized Rindler-like modes which are thermally entangled across each null surface, much like in Minkowski spacetime [12]. The Boltzmann factor controlling this thermal entanglement suppresses only high Rindler-frequency modes. However, for a fixed Rindler frequency, there are a logarithmically infinite number of modes supported arbitrarily close to the entangling surface. (Of course, their small support implies large Minkowskian energy and momentum orthogonal to the entangling surface.) Thus, these modes make at least a logarithmically infinite contribution to entanglement entropy and the mutual information of adjacent subregions. One expects there also to be infinite contributions from other modes with large momenta in directions along the entangling surface.



Figure 1: Deformation of the entangling surface separating R_1 and R_2 along a null congruence.

counterterms, leaving renormalized entropies and mutual information which are finite in smooth states [13]. From here on, we will be referring to these renormalized quantities.

A crucial point is that renormalized entropy S and mutual information I can be made arbitrarily negative² by disentangling short-distance degrees of freedom across the entangling surfaces. What are the consequences of doing so? Our purpose will be to answer this question in terms of energy and its backreaction on spacetime geometry. Serving as our bridge from quantum information will be the quantum null energy condition (QNEC) and quantum focusing conjecture (QFC) [14, 8], which are the successors of the classical null energy condition (NEC) and focusing theorem.

3 The QNEC and the QFC

Though originally formulated in terms of entropy, let us instead state the QNEC and QFC in terms of mutual information. As illustrated in fig. 1, we consider two spatial subregions R_1 and R_2 sharing a portion of their boundaries, which we refer to as the entangling surface. From the entangling surface, an orthogonal congruence of null geodesics³ is generated by a null affine vector field k . Let us call the corresponding affine parameter along the null lines λ and coordinatize spatial directions in the null congruence by y^i . The entangling surface is a spatial section of the congruence specified by a function $\lambda(y)$ and has an induced metric $h_{ij}(y, \lambda(y))$. We can then consider deforming R_1 and R_2 such that the entangling surface $\lambda(y)$ moves along the null congruence. In this way, the mutual information $I_{R_1:R_2}$ can be

²Having a negative renormalized entropy or mutual information between adjacent subregions often indicates that one has begun probing (in this case, disentangling) degrees of freedom shorter than the renormalization distance scale. One may wish instead to set a renormalization distance scale shorter than all degrees of freedom under consideration; in this case, the renormalization scale is similar to a cutoff scale and, as we consider ever shorter distances, renormalized quantities, such as entropy in smooth states, become large similar to bare quantities. What will be important to us is only that entropy and mutual information for adjacent subregions can be decreased by an arbitrarily large amount relative to smooth states by disentangling degrees of freedom at arbitrarily short distances. For succinctness, we will fix a finite renormalization scale and say that renormalized entropy or mutual information becomes arbitrarily negative. (This is, of course, up until the field theory description breaks down, such as at the Planck scale. See footnote 4.)

³In the original version of this essay, the word “lightsheet” was used as a colloquial synonym for a congruence of null geodesics orthogonal to a spatial codimension-two hypersurface. However, this word already has a specialized meaning [15] which we do not want to evoke.

viewed as a functional $I[\lambda]$, whose variation appears in the QNEC and QFC.

In particular, the QNEC [8, 14] states that the null component of the quantum field stress tensor expectation value is bounded from below,

$$\langle T_{kk}(y, \lambda(y)) \rangle \geq \frac{1}{4\pi \sqrt{h(y, \lambda(y))}} \frac{\delta^2 I[\lambda]}{\delta \lambda(y)^2}, \quad (3)$$

by the diagonal piece of the second variation,

$$\frac{\delta}{\delta \lambda(y_2)} \frac{\delta I}{\delta \lambda(y_1)} = \frac{\delta^2 I}{\delta \lambda(y_1)^2} \delta(y_1 - y_2) + \left(\frac{\delta}{\delta \lambda(y_2)} \frac{\delta I}{\delta \lambda(y_1)} \right)_{\text{off-diag}}. \quad (4)$$

(The off-diagonal piece is non-positive, simply by the strong subadditivity property of entropy [8].) The classical limit of QNEC is the classical NEC $T_{kk} \geq 0$ which leads to the focusing theorem $\partial_\lambda \theta \leq 0$ governing the classical expansion

$$\theta(y, \lambda) = \frac{1}{\sqrt{h(y, \lambda)}} \frac{\partial \sqrt{h(y, \lambda)}}{\partial \lambda} = \frac{1}{\sqrt{h(y, \lambda)}} \frac{\delta A[\lambda]}{\delta \lambda(y)}, \quad (5)$$

in the area A of the spatial sections of the null congruence. Similarly associated to the QNEC is the QFC [8] governing a quantum expansion,

$$\frac{\delta \bar{\Theta}[\lambda](y_1)}{\delta \lambda(y_2)} \leq 0, \quad \bar{\Theta}[\lambda](y) = \theta(y, \lambda(y)) + \frac{2G_N}{\sqrt{h(y, \lambda(y))}} \frac{\delta I[\lambda]}{\delta \lambda(y)}. \quad (6)$$

The QNEC and QFC have provided invaluable connections between quantum information and the more familiar notions of energy and geometry encountered in semiclassical gravity, notably in black hole and cosmological contexts [8, 16, 17, 18]. When gravity is holographically dual to a theory on its boundary, the QNEC and QFC in gravity are inextricably tied to consistency conditions in the boundary theory [19, 20]. Moreover, as a statement purely in QFT, the QNEC has been independently proven in a variety of settings [21, 14, 22].

Below, we will apply the QNEC and QFC to situations where significant entanglement is broken between degrees of freedom at short distances. A minor caveat is that the QNEC (3) is only expected to hold at points of the null congruence with vanishing expansion θ and shear [8, 20]. However, we will be more generally extrapolating the lessons we learn from it at short-distances, where background curvature should not significantly alter our qualitative results. In contrast, the QFC and our arguments based on it have no such caveat.

4 Disentanglement and its consequences

Using the QNEC and QFC, we now argue that infinite energies and strong spacetime singularities become inevitable once certain disentanglement criteria are met. In particular, we study situations where degrees of freedom in R_1 and R_2 become increasingly disentangled as the entangling surface is pushed towards a given spatial section $\lambda_0(y)$ of the previously introduced null congruence. Considering a one parameter family of entangling surfaces $\lambda_\alpha(y)$

moving monotonically $\partial_\alpha \lambda_\alpha \geq 0$, our disentanglement criteria will dictate the bad behaviour of mutual information $I[\lambda_\alpha]$ as $\alpha \rightarrow 0^-$.

More precisely, it follows from the QNEC (3) that the following three conditions cannot simultaneously hold⁴:

- (i) the disentanglement criterion $\partial_\alpha I[\lambda_\alpha] \Big|_{\alpha \rightarrow 0^-} = -\infty$,
- (ii) regularity $\partial_\alpha I[\lambda_\alpha] \Big|_{\alpha'} > -\infty$ at some $\alpha' > 0$, and
- (iii) the finiteness of null energy $\int_{0^-}^{\alpha'} d\alpha \int dy (\partial_\alpha \lambda_\alpha)^2 \sqrt{h} \langle T_{kk} \rangle < +\infty$ in the region bounded by $\lambda_0(y)$ and $\lambda_{\alpha'}(y)$.

Thus, if we assume that the spacetime and state has an extension beyond the disentangling surface λ_0 that is sensible — in particular, satisfying (ii) — then there must be infinite energy present. Of course, this is a contradiction if “sensible” also means having finite energy.

From the QFC (6), we can deduce an analogous set of inconsistent conditions. They are most cleanly stated by choosing the family of entangling surfaces such that the combination $\sqrt{h(y, \lambda_\alpha(y))} \partial_\alpha \lambda_\alpha(y)$ is independent of α . Then, we find that the disentanglement criterion (i) also cannot hold simultaneously with

- (iv) regularity $\partial_\alpha (A + 2G_N I)[\lambda_\alpha] \Big|_{\alpha'} > -\infty$ at some $\alpha' > 0$, and
- (v) finite expansion $\partial_\alpha A[\lambda_\alpha] \Big|_{\alpha \rightarrow 0^-} < +\infty$ at λ_0 .

Moreover, if, instead of statement (i), one has

- (i') the stronger disentanglement criterion $I[\lambda_{0^-}] - I[\lambda_{\alpha''}] = -\infty$ for some $\alpha'' < 0$,
- then statement (v) can likewise be replaced by the requirement of
- (v') finite area $A[\lambda_{0^-}] - A[\lambda_{\alpha''}] < +\infty$.

In any case, the interpretation parallels that of statements (i) to (iii). Initially supposing an extension beyond the disentangling surface λ_0 which is sensible — in particular, satisfying statement (iv) — we are invariably led to the contradictory conclusion that a geometric singularity lives at λ_0 . This singularity is so strong that the putative extension of the spacetime cannot solve the gravitational equations of motion even in a weak sense.

We have thus made concrete the notion that sufficient disentanglement leads to infinite energies and strong singularities in backreacted spacetimes. There are many examples, known for some time, of states with infinite energies associated to disentanglement. These include Rindler vacua [23, 7] and states produced by joining quenches of initially disentangled subsystems [24, 25, 26].⁵ The latter are closely related to even earlier work on Lorentzian backgrounds undergoing topology change [27], where the resulting infinite energies were argued to violently abort such processes. In similar spirit, we will apply the disentanglement criteria identified above to argue that strong singularities develop at black hole Cauchy horizons, effectively aborting the spacetime just short of the unpredictable region beyond.

⁴In this essay, we are studying entanglement at very short distances. Going to ever short distances, eventually, the field theory description of physics will break down, *e.g.* due to quantum gravity near the Planck scale. In this essay, writing “ ∞ ” will often come with this caveat.

⁵In appendix A.1, we review the example of a joining quench for a two-dimensional CFT. Conformal symmetry is sufficient to permit the explicit calculation of the stress tensor, entropy, and mutual information, while being agnostic to the particular choice of CFT. We see that our disentanglement criterion (i) (and even the stronger criterion (i'), though gravity is not dynamical in this example) is satisfied on a horizon emanating from the joint. Living on this horizon is also a null energy shock wave that takes the form of a positive, non-integrable contact term.

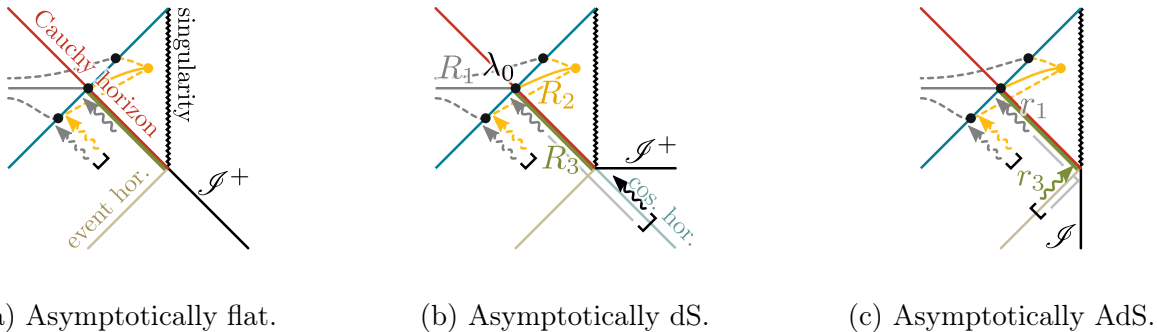


Figure 2: Black holes with Cauchy horizons.

5 Strong cosmic censorship

Let us consider semiclassical theories of matter and gravity on black hole backgrounds which possess Cauchy horizons. Some examples are illustrated in fig. 2, but our discussion can be easily generalized to other cases, including evaporating and rotating black holes. Naively, it may appear that the background and quantum fields can be extended beyond the Cauchy horizon, but this would be problematic as such extensions are not uniquely determined by the initial data or state on a full time slice in the far past. The strong cosmic censorship (SCC) proposal instead suggests that strong singularities must cut off the spacetime at (or before) the Cauchy horizon.

Over half a century ago, Penrose [28] first argued classically for SCC by appealing to the arbitrarily strong blue-shift affecting perturbations falling into the black hole at late times. This is thought to result in signals carrying arbitrarily large energy, illustrated by the first wavy arrow r_1 immediately below each Cauchy horizon in fig. 2, which sources a spacetime singularity enforcing SCC. Unfortunately, counterexamples exist in asymptotically de Sitter (dS) spacetimes. Here, a competing cosmological red-shift can weaken the aforementioned effect such that the spacetime may admit an extension beyond the Cauchy horizon [29, 30]. Fortunately, at the semiclassical level, the quantum stress tensor diverges sufficiently strongly to restore SCC in certain situations such as Reissner-Nordström-dS, as verified by direct calculation [10]. Surprising exceptions persist semiclassically in certain anti-de Sitter (AdS) black holes [31, 32, 11], but these do not seem to survive small changes to the theory or background [33, 34].

Using our disentanglement criteria, we will now provide an exceedingly general study of SCC in black holes of arbitrary spacetimes. Previously, the authors of [11] derived entanglement criteria necessitated by smooth Cauchy horizons that can be evaluated using free field modes on a given background. In contrast, we will argue in a more physically transparent way for our disentanglement criteria, without reliance on any explicit calculations and being largely insensitive to details of the background. Cauchy horizons satisfying our disentanglement criteria not only fail to be smooth, but are sufficiently singular to enforce SCC, as we now explain.

Let us demonstrate SCC by contradiction: suppose that there is some sensible candidate extension beyond the Cauchy horizon. Then, we may consider the mutual information I between the regions R_1 and R_2 shown respectively in grey and yellow in fig. 2. As illustrated

there, we deform R_1 and R_2 such that the black entangling surface between them is pushed along the blue null congruence through the red Cauchy horizon. We will soon argue that, with the possible exception of special cases in AdS, our disentanglement criteria (i') and thus (i) are satisfied at the intersection λ_0 of the null congruence with the Cauchy horizon (*i.e.*, the middle black dots in fig. 2). As part of being “sensible”, we expect that the geometry and state are not persistently singular above the Cauchy horizon, so that the regularity conditions (ii) and (iv) are eventually met. However, the QNEC and QFC then imply the presence of infinite energy and a strong spacetime singularity, in violation of conditions (iii), (v) and (v'). As previously described, such singularities are too severe to recover (even weak) solutions to the gravitational equations of motion, thus enforcing SCC.

6 Disentanglement across the Cauchy horizon

It remains to argue that the mutual information $I_{R_1:R_2}$ does indeed become $-\infty$ across the entangling surface λ_0 on the Cauchy horizon. To make any progress, we must confront the uncertain physics introduced by the high curvature region near the naive black hole singularity, drawn as zigzags in fig. 2. However mysterious the dynamics may be, we nonetheless expect there to be some evolution — more precisely, a quantum channel — relating the state on the portion R_3 of the Cauchy horizon below λ_0 to the state on R_2 . In fig. 2, we have drawn R_3 in green. This precludes, for example, the perverse possibility for the black hole singularity to magically re-emit into R_2 bits of quantum information previously absorbed by the future asymptotic boundary \mathcal{I}^+ . Certainly, our knowledge of semiclassical gravity may be insufficient to *determine* the evolution $R_3 \rightarrow R_2$; we are assuming merely that such a channel *exists*. Since mutual information is monotonic $I_{R_1:R_3} \geq I_{R_1:R_2}$ through quantum channels, it will suffice to argue that $I_{R_1:R_3}$ is negatively divergent.⁶

The culprits behind this entanglement deficit are the same infinitely many, arbitrarily energetic degrees of freedom $r_1 \subset R_1$ that Penrose prophetically identified in his original argument.⁷ Here, however, these degrees of freedom need not be excited outside the black

⁶Below, we present an argument based on physical intuition about the entanglement carried by QFT degrees of freedom. In appendix A.2, we explicitly calculate the mutual information $I_{R_1:R_3}$ for two-dimensional CFTs in arbitrary stationary black holes. The conclusions of our intuitive argument below for asymptotically flat, dS, and AdS black holes are all precisely reproduced. We also calculate the CFT stress tensor and compare mutual information to this more standard probe of SCC.

⁷When the fields are free in the ultraviolet, these degrees of freedom can be precisely identified as the local Rindler-like modes constructed by [11], which we describe in footnote 1. The important point is not only that there are infinitely many of these modes, but also that they would ordinarily, in a smooth state, make an infinite contribution to the mutual information between adjacent subregions.

An interesting point is that this is a logarithmic infinity, as mentioned in footnote 1, such that the disentanglement of these modes results in a deficit in mutual information $I_{R_1:R_2}$ (or $I_{R_1:R_3}$ as specified in appendix A.2) which diverges logarithmically in the affine separation $\lambda_0 - \lambda$ between the Cauchy horizon and the entangling surface. Meanwhile, in more standard approaches to probing SCC, the stress tensor has been found to diverge quadratically with respect to the Kruskal coordinate across the inner horizon, sometimes negatively — see, *e.g.* [10]. The strength of this divergence is therefore compatible with the QNEC (3) and the logarithmic entanglement deficit of the Rindler-like modes. In appendix A.2.3, studying two-dimensional CFTs, we quantitatively examine this relationship between mutual information and the stress tensor near the Cauchy horizon.



Figure 3: Infinitely entangled excitations r'_1 and r_3 produce divergences in entropy S_R .

hole from the local vacuum as in the classical case. As we will elaborate, what concerns us is that the infinitely many degrees of freedom in r_1 do not seem to be entangled with degrees of freedom in R_3 and thus R_2 . This can be contrasted with analogous degrees of freedom (dashed wavy arrows in fig. 2) entangled across earlier choices of the entangling surface $\lambda_{\alpha < 0}$, where they make an infinite positive contribution (balanced by counterterms) in $I_{R_1:R_2}[\lambda_{\alpha < 0}]$. We will now argue that it is impossible to make up for the potentially missing analogous entanglement across λ_0 , except in some AdS cases.

Let us proceed by supposing the contrary, that the entanglement budget is balanced by infinite entanglement between some degrees of freedom $r'_1 \subset R_1$ and $r_3 \subset R_3$ so that $I_{R_1:R_3} > -\infty$. A priori, r'_1 need not be the same as r_1 . However, any such $r'_1 \neq r_1$ must constitute infinite energy excitations, as we now explain by tracking these degrees of freedom back in time. The infinite entanglement carried by r'_1 , which compensates for r_1 at R_1 , must also contribute to the renormalized entropies of earlier subregions in the interior of the spacetime region away from the Cauchy horizon — we illustrate this in fig. 3. As shown, we may apply the QNEC and QFC to the light-blue null congruence which crosses the path of these excitations (with entropy $2S$ replacing mutual information I in eqs. (3) and (6)). Due to the infinite entanglement carried by the excitations, the QNEC and QFC imply that they must also carry infinite energy and thus regrettably imprint a strong singularity on spacetime. To keep the spacetime intact up to the Cauchy horizon, we must therefore make do with $r'_1 = r_1$.

The above considerations highlight a more general point: at least prior to approaching the Cauchy horizon, the infinite entanglement between $r'_1 = r_1$ and r_3 must be attributed to the correlations in locally vacuum-like fluctuations, as opposed to excitations. As previously mentioned, the former type of entanglement is renormalized by counterterms in entropy and mutual information, so the disastrous conclusions drawn from the QNEC and QFC in the previous paragraph would be nullified. However, due to the short-distance nature of such entanglement, (nearly all of) the degrees of freedom r_1 and r_3 must have travelled closely together up to the Cauchy horizon. The final, kinematical puzzle is how this can be achieved, given the ultrarelativistically infalling momenta carried by r_1 , and the parametrically different momenta⁸ of r_3 required to cross R_3 .

⁸As a toy analysis, one can consider timelike and null geodesics in a static black hole as geometric approximations to the trajectories of localized free field modes. Considering the sign of the conserved quantity associated to the static Killing vector, it is easy to see that no null or timelike geodesics connect the (right) event horizon to the (right) Cauchy horizon. In other words, a particle in fig. 2 that fell across the event horizon, *e.g.* closely following r_1 , will carry too much inertia to freely cross R_3 . Such a simple argument may not exist more generally, but the degrees of freedom r_1 always carry parametrically large infalling momenta — see footnotes 1 and 7 — such that they should not cross the Cauchy horizon arbitrarily

With the absence of any conceivable resolutions in asymptotically flat and dS spacetimes, the argument is complete in these cases. In fact, the dS argument can be further strengthened. Tracking r_1 back in time, as illustrated in fig. 2b, we realize that r_1 must be entangled across the cosmological horizon to degrees of freedom captured by \mathcal{S}^+ — otherwise, we would be running a disentanglement argument for a singular cosmological horizon instead of the Cauchy horizon. Calculations with free fields also show this explicitly for smooth states [35]. What remains unappreciated⁹, however, is the monogamous nature of entanglement, which forbids r_1 from further entangling with other partners r_3 . Thus, the putative entanglement between r_1 and r_3 is forbidden by both kinematics and entanglement monogamy.¹⁰

In contrast, the AdS asymptotic boundary \mathcal{S} allows the degrees of freedom r_1 to dramatically change their kinematics by bouncing off.¹¹ Tracking r_1 back in time, we see in fig. 2c that these degrees of freedom were formerly Hawking radiation emitted near the black hole event horizon. Again, to avoid an earlier singularity here, they must be entangled with partners across the horizon — this is famously connected to the information paradox [6]. But in contrast to dS, we see in fig. 2c that these partners land in R_3 and we may be able to identify them as the sought after r_3 . Thus, our analysis remains inconclusive for AdS, which is a somewhat comforting check that we have not cheated.¹² After all, strong singularities appear to be absent at the Cauchy horizons in some special AdS black holes [31, 32, 11] (but apparently reappear with slight changes to the theory or background [33, 34]).

shortly above λ_0 .

⁹I thank Stefan Hollands for discussing this point with me.

¹⁰For two-dimensional CFTs on arbitrary stationary black hole backgrounds, we show in appendix A.2.3 that $I_{R_1:R_3}$ indeed diverges negatively in asymptotically flat and dS cases. When considering Unruh states with cosmological radiation falling into the black hole, the coefficient of the divergence in the stress tensor vanishes when the temperature of the infalling radiation matches the inner horizon temperature (in agreement with [10]). In contrast, the divergence in $I_{R_1:R_3}$ is unaffected by the infalling radiation, as predicted by the above discussion about the capture of entangled partners by \mathcal{S}^+ . This illustrates how mutual information can serve as a more refined probe of SCC than local observables such as the stress tensor.

¹¹This paragraph is about reflecting boundary conditions at the AdS boundary \mathcal{S} . Instead, one may, for example, couple the asymptotically AdS spacetime to a bath, where \mathcal{S} is a transparent interface between the two systems — see, *e.g.* [3, 17]. In such cases where outgoing degrees of freedom are not reflected into the black hole, the situation is more akin to an asymptotically flat or dS black hole, so we do expect the Cauchy horizon to satisfy our disentanglement criteria.

¹²In appendix A.2.3, we calculate the mutual information $I_{R_1:R_3}$ for CFTs in two-dimensional asymptotically AdS black holes in the Hartle-Hawking state. The logarithmic divergence of this mutual information has a coefficient which is negative, zero, or positive, depending on whether the outer horizon temperature is less than, equal to, or greater than the inner horizon temperature. The stress tensor diverges quadratically (in inner horizon Kruskal coordinates) with a coefficient that is different, but also fits this description.

While our disentanglement criteria only holds for a range of temperatures, positively divergent mutual information and entropies are also dangerous due to the QNEC and QFC, as briefly mentioned at the end of appendix A.2.3. It would be worthwhile to obtain a general explanation of when disentanglement or hyper-entanglement occurs at the Cauchy horizons in AdS black holes. This may then provide an intuitive argument for strongly singular Cauchy horizons with the exception of a measure-zero set of parameters, thus generically securing SCC in AdS black holes. (However, as [11] points out, the fate of SCC in AdS black holes may yet be obscured by very bizarre phenomena appearing at late boundary times, such as tunnelling by wormhole emission [36].)

7 Conclusion

By appealing to the QNEC and QFC, we have concretely related the destruction of entanglement to the presence of infinite energies and strong spacetime singularities. The power of these ideas was demonstrated by giving an exceedingly general and physically transparent explanation of SCC for quantum fields in semiclassical black holes. While the causal structure of spacetime clearly dictates the flow of entanglement, we have conversely seen how regions starved of entanglement are rejected from spacetime. It is intriguing that gravity is so inextricably codependent on quantum information.

Acknowledgements

I am grateful to Stefan Hollands, Gary T. Horowitz, Maciej Kolanowski, Donald Marolf, Arvin Shahbazi-Moghaddam, and Marija Tomašević for helpful discussions. I would like to thank the Institute for Advanced Study for its support and hospitality during the Workshop on Spacetime and Quantum Information held on December 11-13, 2023. I am supported by a Fundamental Physics Fellowship through the University of California, Santa Barbara.

A Energy and entanglement in two-dimensional CFTs

In the intuitive spirit of this essay, thus far, we have maintained a rather qualitative level of discussion about the entanglement and disentanglement between QFT degrees of freedom. The goal of this appendix is to supplement the intuition we have developed in the main body of this essay with quantitative examples. For simplicity, we reduce attention to conformal field theories (CFTs) in two spacetime dimensions.

While the metric has no propagating degrees of freedom in two dimensions, one can consider toy models of gravity, *e.g.* Jackiw-Teitelboim (JT) gravity, by introducing other “geometric” degrees of freedom, *e.g.* a dilaton. The role played by area in connection to entropy and the QFC is then taken up by these degrees of freedom, so our analysis in section 4 should have generalizations to such toy models¹³. Since our focus is on field theory in this appendix, however, we will consider only CFTs on fixed background metrics.

In these two-dimensional CFTs, we will be able to calculate the stress tensor, entropy, and mutual information explicitly. Leveraging conformal and Weyl transformations, we will be able to perform these calculations while being completely agnostic to the chosen CFT — it may be free or strongly interacting, contain one or many fields. In appendix A.1, we review the example of a joining quench, where the infinite energy accompanying disentanglement can be calculated in a regulated manner. Next, in appendix A.2, we examine CFTs on arbitrary stationary black hole backgrounds. We evaluate the mutual information $I_{R_1:R_3}$ for the regions R_1 and R_3 which played starring roles in our argument for disentanglement across

¹³JT gravity has been extensively dissected as a toy model for gravity in the context of the black hole information paradox, as initiated by [3]. The QFC has been used in this context to avoid some auxiliary paradoxes [17]. See [34] for a discussion of two-dimensional dilaton theories with respect to SCC.

Cauchy horizons in section 6. This will provide opportunities to compare our approach with other approaches to probing SCC based on divergences in the stress tensor.

A.1 A joining quench example

As shown in fig. 4a, we consider a joining quench of two half-spaces [24, 25, 26]¹⁴. In the lower half of fig. 4a, the two half-spaces — $\mathbb{R}_{<0}$ and $\mathbb{R}_{>0}$ respectively \times time — are initially unentangled and separated by a wall where reflecting boundary conditions are imposed. For concreteness, let us prepare each of the half-spaces in the vacuum state, where the stress tensor $\langle T_{\mu\nu} \rangle = 0$ vanishes. At a given time $t = 0$, the two half-spaces are then joined suddenly by removing the wall separating them. We will calculate the stress tensor and mutual information in this more complicated setup by analytic continuation from Euclidean signature.

In the top panel of fig. 4b, we have illustrated the flat Euclidean geometry, with complex coordinates (z, \bar{z}) , over which a path integral prepares, up to a regulator ε , the aforementioned half-space vacua product state on the $(-z + \bar{z})/2 = 0$ time slice. As shown, an extra ε amount of Euclidean evolution has been applied to the state, with the wall removed. As we will see, this regulates the otherwise infinite energy of the joined state by exponentially $e^{-\varepsilon E}$ suppressing high energy E eigenstates of the joined, *i.e.* Minkowski, Hamiltonian. Moreover, it has the effect of reconstructing the Minkowski vacuum entanglement between degrees of freedom in the two half-spaces at energies $\gtrsim 1/\varepsilon$, while leaving lower energy degrees of freedom untouched in the half-space vacua.

The conformal transformation

$$w = i\sqrt{\frac{i\varepsilon + z}{i\varepsilon - z}} \quad (7)$$

maps the geometry in the top panel of fig. 4b to the w upper-half-plane, as shown in the bottom panel. In this half-space geometry, the stress tensor again vanishes. Moreover, as we will describe further below, entanglement entropies and mutual information can be evaluated using the half-space correlation functions of twist operators. These answers can then be conformally mapped through eq. (7) and analytically continued to the Lorentzian spacetime in fig. 4a, where (z, \bar{z}) are null coordinates.

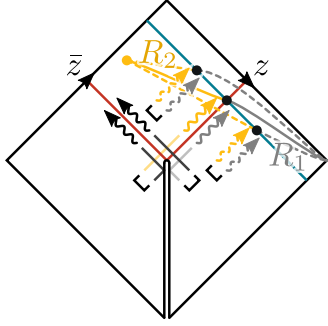
The resulting stress tensor is¹⁵

$$\langle T_{zz} \rangle = -\frac{c}{24\pi} \{w, z\} = \frac{c\varepsilon^2}{16\pi(z^2 + \varepsilon^2)^2}. \quad (8)$$

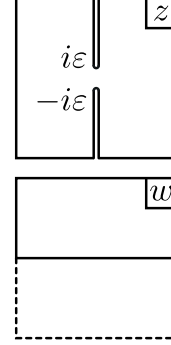
Here, c is the central charge of the CFT, and $\{w, z\}$ is the Schwarzian derivative. In the limit $\varepsilon \rightarrow 0$, we see that $\langle T_{zz} \rangle$ becomes a non-integrable contact term $+\infty \delta(z)$ at the right

¹⁴Joining quenches have also played a part in considerations of the black hole information paradox, where an AdS black hole is joined to a bath which collects Hawking radiation. See, *e.g.* [3], which also provides a reasonable review of CFT entanglement entropy calculations as well as the connection to twist operators, boundaries, conformal transformations, and Weyl transformations — ideas which we will make use of.

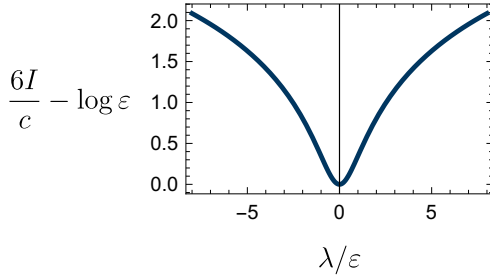
¹⁵A direct analytic continuation, as written here, describes a time-reversal-symmetric Lorentzian evolution where the wall is removed to both the future and the past. This differs from the physical evolution illustrated in fig. 4a only in the causal past of the joint $z = \bar{z} = 0$ (in the $\varepsilon \rightarrow 0$ limit).



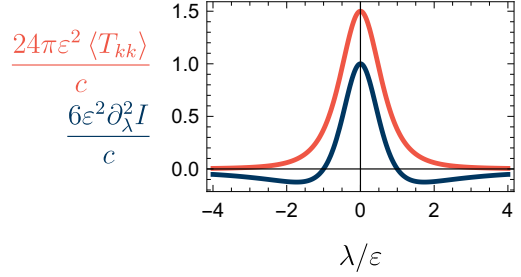
(a) Two half-spaces, initially in their vacuum states and separated by a wall, are suddenly joined. The joint produces null energy shock waves (red), across which certain degrees of freedom (solid grey and yellow wavy arrows) are entangled not with each other, but far away partners (black wavy arrows).



(b) The CFT state can be prepared by a Euclidean path integral over the geometry in the top panel, which can then be conformally mapped by eq. (7) to the upper-half-plane in the lower panel.



(c) Renormalized mutual information $I_{R_1:R_2}$ plotted against the affine parameter $\lambda = -z_e$ at the entangling surface (z_e, \bar{z}_e) along the blue null line in (a). The yellow endpoint in (a) is chosen to be at $\bar{z}_2 = 1/2$, while the plot is independent of the choices of \bar{z}_e and z_2 .



(d) The stress tensor expectation value and the second derivative of mutual information. The QNEC (16) states that the red curve is bounded from below by the dark blue curve.

Figure 4: Disentanglement from a joining quench.

red horizon in fig. 4a. The anti-holomorphic component of the stress tensor similarly reduces to an infinite energy shock wave $+\infty \delta(\bar{z})$ localized on the left horizon. In addition to analogous contact terms, the stress tensor for Rindler vacua also has a power law divergence as one approaches the horizon [23]. As we elaborate below, what our joining quench example illustrates is that disentanglement need not be accompanied by a stress tensor that diverges *on approach* to the disentanglement surface as for Rindler vacua; the infinite energy deduced in section 4 can be localized at the disentanglement surface.

To quantify disentanglement and study the QNEC, we next consider mutual information (2) between the grey R_1 and yellow R_2 regions in fig. 4a whose black entangling surface (or rather, point) slides along the blue null line. Let us denote the coordinates of the yellow left endpoint of R_2 and the black entangling surface respectively by (z_2, \bar{z}_2) and (z_e, \bar{z}_e) .

As part of the mutual information $I_{R_1:R_2}$, we will need the entropies

$$S_{R_1} = S^{\mathbb{C}/\mathbb{Z}_2}(w(z_e), \bar{w}(\bar{z}_e)) - \frac{c}{6} \log \sqrt{w'(z_e)\bar{w}'(\bar{z}_e)}, \quad (9)$$

$$S_{R_1 \cup R_2} = S^{\mathbb{C}/\mathbb{Z}_2}(w(z_2), \bar{w}(\bar{z}_2)) - \frac{c}{6} \log \sqrt{w'(z_2)\bar{w}'(\bar{z}_2)}, \quad (10)$$

where¹⁶

$$S^{\mathbb{C}/\mathbb{Z}_2}(w, \bar{w}) = \frac{c}{6} \log \left(\frac{w - \bar{w}}{i} \right) + \log g \quad (11)$$

derives from the one-point function of a twist operator in the w half-plane. The other terms in eq. (9) result from the conformal transformation $w \mapsto z$ mapping this twist insertion to the single endpoints of the regions R_1 and $R_1 \cup R_2$. In the w half-plane, conformal invariance determines one-point functions up to normalization, manifesting as the boundary entropy $\log g$ above [37] — this constant will cancel out below.

Unfortunately, also appearing in $I_{R_1:R_2}$ is the entropy S_{R_2} of the region R_2 with two endpoints, corresponding to a two-point function of twist operators. While this is not determined by conformal invariance in general, the limit $\varepsilon, |z_e| \ll \bar{z}_e, -z_2, \bar{z}_2$ where the entangling surface is close to the red horizon in fig. 4a corresponds to an operator product expansion (OPE) limit of the twist operators in the w half-plane. In this limit, the w half-plane two-point function is well approximated by a full-plane two-point function¹⁷, so that

$$S_{R_2} \sim S^{\mathbb{C}}(w(z_e), \bar{w}(\bar{z}_e); w(z_2), \bar{w}(\bar{z}_2)) - \frac{c}{6} \log \sqrt{w'(z_e)\bar{w}'(\bar{z}_e)w'(z_2)\bar{w}'(\bar{z}_2)} \quad (13)$$

¹⁶We are considering renormalized entropies here. Their bare quantities corresponding to eqs. (11) and (14) have divergences $\frac{c}{6} \log(\epsilon)$ and $\frac{c}{6} \log(\epsilon^2)$ logarithmic in the ultraviolet cutoff ϵ of the CFT (not to be confused with the ε regulator of the shock wave).

¹⁷By the method of images, the half-plane two-point function of twist operators is similar to a full-plane four-point function. Thus, it is controlled by a cross-ratio

$$\eta(w_1, \bar{w}_1; w_2, \bar{w}_2) = -\frac{(w_1 - \bar{w}_1)(w_2 - \bar{w}_2)}{(w_1 - w_2)(\bar{w}_1 - \bar{w}_2)}. \quad (12)$$

(In the present case, the relevant cross-ratio is $\eta(w(z_e), \bar{w}(\bar{z}_e); w(z_2), \bar{w}(\bar{z}_2))$ where w is given by eq. (7).) The limit $\eta \rightarrow \infty$ corresponds to the OPE limit where the half-plane two-point function of twist operators is approximated by a full-plane two-point function and the corresponding expression for entropy is eq. (14). See, *e.g.* [3] (but note that we are using a different cross-ratio and our boundary is at $w = \bar{w}$).

where

$$S^{\mathbb{C}}(w_1, \bar{w}_1; w_2, \bar{w}_2) = \frac{c}{6} \log [(w_1 - w_2)(\bar{w}_1 - \bar{w}_2)] . \quad (14)$$

Collecting the pieces and simplifying using the limit $\varepsilon, |z_e| \ll \bar{z}_e, -z_2, \bar{z}_2$, we find

$$I_{R_1:R_2} \sim \frac{c}{6} \log \left[\frac{\sqrt{\varepsilon^2 + z_e^2} (\bar{z}_e - \bar{z}_2) \bar{z}_e}{\bar{z}_2} \right] . \quad (15)$$

Using $k = -\partial_z$ and $\lambda = -z_e$ as the affine generator and parameter along the blue null line, the two-dimensional QNEC states that

$$\langle T_{zz}(z_e) \rangle = \langle T_{kk}(z_e) \rangle \geq \frac{1}{4\pi} \partial_\lambda^2 I_{R_1:R_2} = \frac{1}{4\pi} \partial_{z_e}^2 I_{R_1:R_2} \quad (16)$$

$$\sim \frac{c}{24\pi} \frac{\varepsilon^2 - z_e^2}{(\varepsilon^2 + z_e^2)^2} . \quad (17)$$

We plot eqs. (8), (15) and (17) in figs. 4c and 4d, where we see that the QNEC is indeed satisfied.

Upon removing the regulator $\varepsilon \rightarrow 0$, the mutual information (15) is negatively, logarithmically divergent as the black entangling surface $\lambda = -z_e$ is pushed towards the red horizon $\lambda_0 = 0$, thus satisfying our disentanglement criterion (i) (and also the stronger criterion (i'), but gravity is not dynamical here). As predicted in section 4, we find infinite energy $\langle T_{kk} \rangle = +\infty \delta(z)$. In the $\varepsilon \rightarrow 0$ limit, eq. (15) is concave-down with respect to $z_e \neq 0$, so one might naively think that the QNEC (16) places no bound on positive energy. However, as made clear in fig. 4d with the ε regulator reinstated, $\partial_\lambda^2 I_{R_1:R_2}$ is large and positive in the region $-\varepsilon \lesssim z_e \lesssim \varepsilon$, where the QNEC then dictates the presence of positive energy.

In the spirit of this essay, let us end this example by sketching an intuitive explanation of the disentanglement across the red horizon. As illustrated in fig. 4a for the right horizon, the culprits are right-moving degrees of freedom (wavy arrows) which are ordinarily (in the dashed cases) infinitely entangled (as indicated by brackets) at short distances across the entangling surface (black dot). However, let us consider the analogous degrees of freedom (solid grey and yellow wavy arrows) across the entangling surface (middle black dot) located on the horizon. Tracing these back in time, we see that the sudden removal of the reflecting wall means that the solid grey and yellow degrees of freedom originate respectively from the right and left half-spaces and should not be infinitely entangled with each other. Rather, given the short-distance entanglement present in each half-space vacuum, they are instead entangled with degrees of freedom (black wavy arrows) which have propagated away and do not contribute to the entanglement between R_1 and R_2 as measured by $I_{R_1:R_2}$.

A.2 Stationary black hole backgrounds

Finally, we consider CFTs on stationary two-dimensional black hole backgrounds,

$$ds^2 = -f(r) dt^2 + \frac{dr^2}{f(r)} . \quad (18)$$

Our goal will be to evaluate the stress tensor and the mutual information for regions relevant to our disentanglement argument for Cauchy horizons, presented in section 6. We begin in appendix A.2.1 by describing the variety of black holes (18) that we will consider and introduce Kruskal coordinates adapted to various horizons in these geometries. Then, in appendix A.2.2 we describe the construction of conformal vacua, corresponding to Unruh and Hartle-Hawking states with no infalling radiation and infalling radiation at various temperatures. We also describe the compatibility of these vacua with the asymptotically flat, dS, and AdS geometries we consider. Finally, in appendix A.2.3, we evaluate the stress tensor and mutual information in these geometries and states.

A.2.1 The geometry and useful coordinates

The curvature of the metric (18) reads

$$R = -f''(r), \quad (19)$$

so the $\sim r^2$ asymptotics of f at large r determine whether the spacetime is asymptotically flat, dS, or AdS at its boundary $r = +\infty$. For relevance to SCC, we consider black holes possessing Cauchy, inner horizons $r = r_- > 0$ in addition to event, outer horizons $r = r_+ > r_-$. For asymptotically dS geometries, there will also be cosmological horizons $r = r_c > r_+$. The blackening factor f then satisfies

$$f(r < r_-) > 0, \quad f(r_- < r < r_+) < 0, \quad f(r_+ < r < r_c) > 0, \quad f(r_c < r) < 0 \quad (20)$$

and vanishes on the horizons,

$$f = \begin{cases} 2\kappa_+(r - r_+) + \mathcal{O}((r - r_+)^2) \\ 2\kappa_-(r_- - r) + \mathcal{O}((r - r_-)^2) \\ 2\kappa_c(r_c - r) + \mathcal{O}((r - r_c)^2) \end{cases} \quad (21)$$

where the $\kappa_{\pm/c}$ denote the respective horizon temperatures. We will not need to specify f any further.¹⁸

Let us clarify that we are not specializing only to dS. Relations involving r_c are only relevant for dS and should otherwise be ignored or modified in the obvious way. In cases other than dS, κ_c will be thought of below as a free parameter, not necessarily determined by geometry as in eq. (21). We will later see that $\kappa_c/2\pi$ describes the temperature of “cosmological” infalling radiation in certain states, whether that be on dS or asymptotically flat spacetimes.

¹⁸There is one more assumption that is needed for the size of the corrections in the stress tensors written below in eqs. (45), (49) and (52). We assume that f admits an expansion near the inner horizon,

$$f = 2a_- \kappa_- z_- \bar{z}_- + b_- (z_- \bar{z}_-)^2 + \mathcal{O}((z_- \bar{z}_-)^3), \quad (22)$$

in terms of the Kruskal coordinates (z_-, \bar{z}_-) and constant a_- introduced below, and another constant b_- . The leading order piece is already expressed in eq. (21). The additional assumption is that the next-to-leading order correction is precisely quadratic and this approximation is accurate up to $\mathcal{O}((z_- \bar{z}_-)^3)$ corrections.

Let us introduce some useful coordinates next. The radial tortoise coordinate r_* is defined by

$$dr_* = \frac{dr}{f}, \quad (23)$$

up to an integration constant that we will not specify — it merely determines the a_{\pm} , a_c , and $R_{\mathcal{J}}$ constants below, which we choose to be all positive. The near-horizon behaviour of r_* reads¹⁹

$$r_* = \begin{cases} \frac{1}{2\kappa_+} \log\left(\frac{r-r_+}{a_+}\right) + \mathcal{O}(r-r_+) \\ -\frac{1}{2\kappa_-} \log\left(\frac{r-r_-}{a_-}\right) + \frac{i\pi}{2\kappa_+} + \mathcal{O}(r-r_-) \\ -\frac{1}{2\kappa_c} \log\left(\frac{r_c-r}{a_c}\right) + \mathcal{O}(r-r_c) \end{cases}. \quad (24)$$

From t and r_* we can define tortoise null coordinates

$$z_t = r_* - t, \quad \bar{z}_t = r_* + t, \quad (25)$$

and Kruskal coordinates²⁰, *e.g.* adapted to the outer horizon,

$$z_+ = e^{\kappa_+ z_t}, \quad \bar{z}_+ = e^{\kappa_+ \bar{z}_t}. \quad (26)$$

There are similar Kruskal coordinates adapted to the inner and cosmological horizons (though not given directly by a substitution of subscripts in eq. (26)). The ranges of various null coordinates are illustrated in fig. 5a. Where the real ranges of any two z or any two \bar{z} Kruskal coordinates overlap in spacetime, the coordinates are related by

$$(-z_+)^{1/\kappa_+} = z_-^{-1/\kappa_-}, \quad \bar{z}_+^{1/\kappa_+} = (-\bar{z}_-)^{-1/\kappa_-}, \quad (27)$$

$$z_+^{1/\kappa_+} = (-z_c)^{-1/\kappa_c}, \quad \bar{z}_+^{1/\kappa_+} = (-\bar{z}_c)^{-1/\kappa_c}, \quad (28)$$

$$(-\bar{z}_-)^{1/\kappa_-} = (-\bar{z}_c)^{1/\kappa_c}. \quad (29)$$

In the case of AdS, the asymptotic boundary is located at finite r_* and thus finite

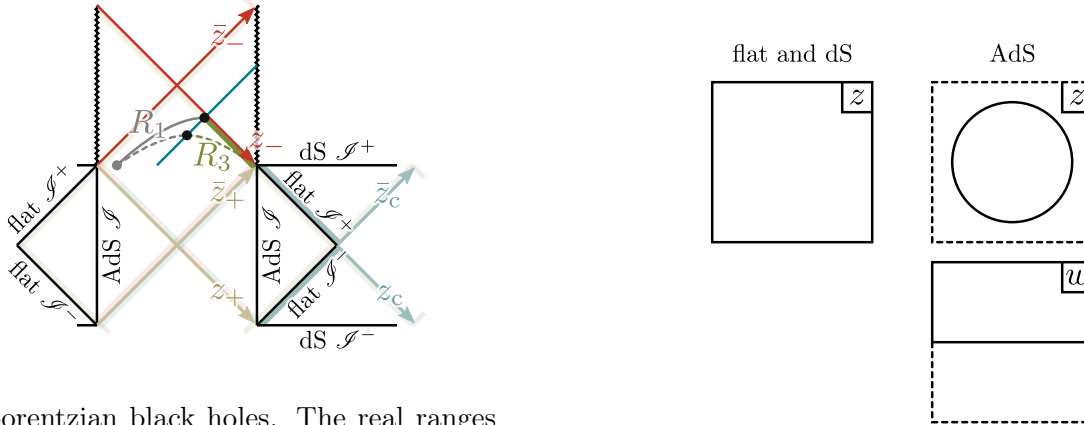
$$z_+ \bar{z}_+ \Big|_{\text{AdS } \mathcal{J}} = R_{\mathcal{J}}^2. \quad (30)$$

The black hole metric (18) becomes conformally flat when written in terms of null coordinates,

$$ds^2 = \frac{dz_I d\bar{z}_J}{\Omega_{IJ}^2}. \quad (I, J \in \{t, +, -, c\} \text{ not summed}) \quad (31)$$

¹⁹Due to the logarithms, $\text{Im } r_*$ jumps discontinuously across each horizon; there are also jumps in $\text{Im } t$ such that the Kruskal coordinates below are defined consistently with respect to t and r_* . We will not dwell on these details, but see *e.g.* [32] for discussion of these imaginary shifts in relation to the Kubo–Martin–Schwinger condition on thermal states. Closely related are eqs. (35) and (36) below.

²⁰Our null tortoise and Kruskal coordinates are related to the more standard ones, often called u , v , U , and V , by $z_t = -u$, $\bar{z}_t = v$, $z_{\pm/c} = -U_{\pm/c}$, and $\bar{z}_{\pm/c} = V_{\pm/c}$. The reasoning behind our conventions will become apparent when we discuss Euclidean state preparation in appendix A.2.2.



(a) Lorentzian black holes. The real ranges $(-\infty, +\infty)$ of the various z and \bar{z} Kruskal coordinates are indicated by lines tipped by arrows at $+\infty$. The tortoise null coordinates z_t and \bar{z}_t are not illustrated; their real ranges correspond respectively to the positive ranges of z_+ and \bar{z}_+ .

(b) The asymptotically flat and dS vacua we consider are prepared on a Euclidean plane. The AdS Hartle-Hawking vacuum is prepared on a disk which can be conformally mapped to the half-plane.

Figure 5: Two-dimensional stationary black holes and the preparation of CFT states.

Of particular interest to us will be the following coordinate pairings,

$$\Omega_{+t}^{-2} = \frac{f}{\kappa_+ z_+} = -\frac{2a_- \kappa_-}{\kappa_+} z_-^{1+\frac{\kappa_+}{\kappa_-}} \bar{z}_- [1 + \mathcal{O}(z_- \bar{z}_-)] , \quad (32)$$

$$\Omega_{+c}^{-2} = -\frac{f}{\kappa_+ \kappa_c z_+ \bar{z}_c} = \frac{2a_- \kappa_-}{\kappa_+ \kappa_c} z_-^{1+\frac{\kappa_+}{\kappa_-}} (-\bar{z}_-)^{1-\frac{\kappa_c}{\kappa_-}} [1 + \mathcal{O}(z_- \bar{z}_-)] , \quad (33)$$

$$\Omega_{++}^{-2} = \frac{f}{\kappa_+^2 z_+ \bar{z}_+} = \frac{2a_- \kappa_-}{\kappa_+^2} z_-^{1+\frac{\kappa_+}{\kappa_-}} (-\bar{z}_-)^{1+\frac{\kappa_+}{\kappa_-}} [1 + \mathcal{O}(z_- \bar{z}_-)] . \quad (34)$$

Above, we have indicated the behaviours of these Weyl factors as the inner horizon is approached from below, expressed in terms of the inner horizon Kruskal coordinates.

A.2.2 State preparation

We turn now to the question of what state we should consider in the CFT. For simplicity, we shall consider three choices of conformal vacua, specified below. However, we also expect that more general states excited above these vacua will behave qualitatively similarly. For example, in a free theory, the authors of [10] considered the difference in the stress tensor expectation value between an Unruh state and an arbitrary other state that is also Hadamard in the same spacetime region. It was shown that this difference has the same regularity as a classical stress tensor when approaching the Cauchy horizon in a black hole. Thus, for the purposes of studying quantum enhancements to SCC, the authors focused on the Unruh state. In similar spirit, we expect the stress tensor and entanglement structure for the CFT states constructed below to also be representative of more general states, at least to leading order near the Cauchy horizon.

Let us now describe the general strategy for constructing our conformal vacua. First, we remove the Weyl factor in the metric eq. (31) so that it becomes flat $dz d\bar{z}$. Next, we continue this flattened geometry to Euclidean signature, where z and \bar{z} now play the role of holomorphic and anti-holomorphic coordinates over a complex plane or a subset of it, as illustrated in fig. 5b and elaborated below. The vacuum state can then be prepared by a path integral over this Euclidean geometry, where we can calculate quantities such as the stress tensor expectation value and entropies. Finally, we continue back to Lorentzian signature and reinstate the Weyl factor in the metric while applying the corresponding Weyl transformations to the quantities we have calculated. The key choice in this procedure is the pair of coordinates z and \bar{z} — different selections from the various null coordinates we have previously identified will result in different vacua.

Hartle-Hawking state at the outer horizon temperature. One choice is the outer horizon Kruskal coordinates (z_+, \bar{z}_+) , which results in the Hartle-Hawking state of the black hole. From eqs. (25) and (26), we see that the statement

$$(z_+, \bar{z}_+) \sim (e^{2\pi i} z_+, e^{-2\pi i} \bar{z}_+) \quad (35)$$

in the Euclidean complex plane corresponds to the identification of time in the thermal circle at the temperature $\kappa_+/2\pi$ of the outer horizon

$$it \sim it + \frac{2\pi}{\kappa_+} . \quad (36)$$

This Hartle-Hawking state is therefore a thermofield double of the left and right exteriors at the outer horizon temperature. The geometry of the complex plane is smooth and, in particular, has no conical singularity at the bifurcation point $z_+ = \bar{z}_+ = 0$, due to eq. (35). Continuing to Lorentzian signature, the Hartle-Hawking vacuum remains smooth over the null ranges covered by the (z_+, \bar{z}_+) Kruskal coordinates. In particular, it is smooth on the maximally extended outer horizon.

Moreover, for asymptotically flat and AdS black holes, this vacuum is smooth over any Cauchy surface (away from the inner horizon) running between the spatial infinities of the left and right exteriors. Among the three vacua we consider, the Hartle-Hawking vacuum is the only one consistent with the reflecting boundary conditions at the asymptotic boundary \mathcal{S} of AdS. The right- and left-moving, *i.e.* holomorphic and anti-holomorphic, degrees of freedom are related here and not independent. Recalling that \mathcal{S} is described by eq. (30), the continuation of the AdS black hole to Euclidean signature is a disk in the complex plane with radius $R_{\mathcal{S}}$. As illustrated on the right in fig. 5b and similar to what we did in appendix A.1, it will be helpful for entropy calculations to consider an additional, Möbius transformation to the upper half plane,

$$w = -i \frac{z_+ + iR_{\mathcal{S}}}{z_+ - iR_{\mathcal{S}}} , \quad \bar{w} = i \frac{\bar{z}_+ - iR_{\mathcal{S}}}{\bar{z}_+ + iR_{\mathcal{S}}} . \quad (37)$$

For dS, except when the outer horizon $\kappa_+/2\pi$ and cosmological $\kappa_-/2\pi$ temperatures match, the Hartle-Hawking state, constructed from (z_+, \bar{z}_+) , will be singular on the cosmological horizon. When the temperatures do match, the Hartle-Hawking state is the same as the Unruh state we consider below.

Unruh state with infalling cosmological radiation. Applying a similar construction to the cosmological Kruskal coordinates (z_c, \bar{z}_c) produces a state that is smooth on the cosmological horizon, but is singular at the black hole outer horizon except when $\kappa_+ = \kappa_c$. Since we are more interested in black holes with smooth outer horizons, we instead opt for a compromise: the Unruh state with outgoing Hawking radiation at temperature $\kappa_+/2\pi$ and infalling cosmological radiation at temperature $\kappa_c/2\pi$. In our CFT context, this Unruh state is the conformal vacuum associated to the (z_+, \bar{z}_c) coordinates. In the Lorentzian geometry, this Unruh state will be smooth in the spacetime regions covered by this pair of Kruskal coordinates. This is similar to the physically relevant parts of the spacetime for a black hole formed by collapse, where the matter covers up the left asymptotic region. This is one reason why the dS Unruh vacuum has been studied, *e.g.* by [10], for the purposes of probing SCC.

In principle, one can also place such a state on asymptotically flat black holes, where there is a shower of radiation at some temperature $\kappa_c/2\pi$ supplied by the right past null infinity \mathcal{I}^- . Here, κ_c is just a free parameter, not determined by geometry (21) as in the dS case.

Unruh state with no infalling radiation. However, perhaps more realistic in this case would be a state where there is no such shower of radiation coming from \mathcal{I}^- . This is the most natural Unruh state for asymptotically flat black holes [12]. Since \bar{z}_t approaches the Minkowski null coordinate $r+t$ on \mathcal{I}^- , this Unruh state is the conformal vacuum associated to (z_+, \bar{z}_t) . Again, the state is smooth on the Lorentzian spacetime regions covered by these null coordinates.

A.2.3 Energy and entanglement

In each of the conformal vacua identified above, we will now calculate the stress tensor expectation value near the Cauchy, inner horizon and the mutual information $I_{R_1:R_3}$ between the regions illustrated in fig. 5a. (The limit where the black entangling surface is placed on the red inner horizon reproduces the regions R_1 and R_3 discussed in section 6.) We will first describe the general calculation of these quantities before presenting the results specific to each state.

To obtain the stress tensor expectation value, we first observe in Euclidean signature that, on the complex plane and the disk with metric $dz d\bar{z}$, the expectation value vanishes. Here, we are bearing in mind some holomorphic and anti-holomorphic coordinates (z, \bar{z}) corresponding to the choice of conformal vacuum, as previously described. Continuing to Lorentzian signature, where (z, \bar{z}) become null coordinates, and reinstating the factor Ω^{-2} in eq. (31) by a Weyl transformation, the stress tensor becomes²¹

$$\langle T_{\bar{z}\bar{z}} \rangle = -\frac{c}{12\pi} \Omega^{-1} \partial_{\bar{z}}^2 \Omega, \quad (38)$$

with a similar T_{zz} component and, of course, a state-independent trace determined by the curvature (19). For relevance to SCC, we are particularly interested in the near-inner-horizon divergences of the stress tensor, which come from the above left-moving component

²¹See, *e.g.* eqs. (6.136) and (6.137) in [38].

as one approaches the right inner horizon in fig. 5a. More precisely, to separate physical divergences from coordinate pathologies, one should transform eq. (38) to a coordinate basis that is regular at the inner horizon, *e.g.* (z_-, \bar{z}_-) . (Let us emphasize that this last step is just a coordinate transformation which leaves the stress *tensor* and metric *tensor* invariant, not a conformal transformation.)

To evaluate the mutual information $I_{R_1:R_3}$, we need the entropies S_{R_1} , S_{R_3} , and $S_{R_1 \cup R_3}$. We will write the coordinates of the left endpoint of R_1 , the entangling surface separating R_1 from R_3 , and the right endpoint of R_3 respectively as (z_1, \bar{z}_1) , (z_e, \bar{z}_e) , and (z_3, \bar{z}_3) , where again we have in mind some choice of null coordinates associated to a given conformal vacuum. We will eventually send (z_3, \bar{z}_3) to the past boundary of the right inner horizon, as illustrated in fig. 5a.

For asymptotically flat and dS black holes, the conformal vacua are prepared on the full complex plane, where the two-point function of twist operators is determined by conformal invariance. After analytic continuation to Lorentzian signature and a Weyl transformation, the resulting entropies are

$$S_{R_1} = S^{\mathbb{C}}(z_1, \bar{z}_1; z_e, \bar{z}_e) - \frac{c}{6} \log [\Omega(z_1, \bar{z}_1)\Omega(z_e, \bar{z}_e)] , \quad (39)$$

$$S_{R_3} = S^{\mathbb{C}}(z_e, \bar{z}_e; z_3, \bar{z}_3) - \frac{c}{6} \log [\Omega(z_e, \bar{z}_e)\Omega(z_3, \bar{z}_3)] , \quad (40)$$

$$S_{R_1 \cup R_3} = S^{\mathbb{C}}(z_1, \bar{z}_1; z_3, \bar{z}_3) - \frac{c}{6} \log [\Omega(z_1, \bar{z}_1)\Omega(z_3, \bar{z}_3)] , \quad (41)$$

where $S^{\mathbb{C}}$ is again given by eq. (14).

For asymptotically AdS black holes, the Hartle-Hawking state is prepared on the Euclidean z disk which can be mapped to the w half-plane — this is illustrated in fig. 5b and described by eq. (37). As previously confronted in appendix A.1, two-point functions in the half-plane are not conformally determined. However, the limit $(z_{3,+}, \bar{z}_{3,+}) \rightarrow (0, +\infty)$ where the right endpoint of R_3 is sent to the past boundary of the right inner horizon, as pictured in fig. 5a, corresponds to sending a twist operator in the w half-plane much closer to the boundary than to other insertions.²² Thus, the half-plane two-point function is well-approximated by one-point functions. Consequently,

$$S_{R_3} \sim S^{\mathbb{C}/\mathbb{Z}_2}(w(z_{e,+}), \bar{w}(\bar{z}_{e,+})) + S^{\mathbb{C}/\mathbb{Z}_2}(w(z_{3,+}), \bar{w}(\bar{z}_{3,+})) - \frac{c}{6} \log \left[\Omega(z_{e,+}, \bar{z}_{e,+})\Omega(z_{3,+}, \bar{z}_{3,+}) \sqrt{w'(z_{e,+})\bar{w}'(\bar{z}_{e,+})w'(z_{3,+})\bar{w}'(\bar{z}_{3,+})} \right] , \quad (42)$$

$$S_{R_1 \cup R_3} \sim S^{\mathbb{C}/\mathbb{Z}_2}(w(z_{1,+}), \bar{w}(\bar{z}_{1,+})) + S^{\mathbb{C}/\mathbb{Z}_2}(w(z_{3,+}), \bar{w}(\bar{z}_{3,+})) - \frac{c}{6} \log \left[\Omega(z_{1,+}, \bar{z}_{1,+})\Omega(z_{3,+}, \bar{z}_{3,+}) \sqrt{w'(z_{1,+})\bar{w}'(\bar{z}_{1,+})w'(z_{3,+})\bar{w}'(\bar{z}_{3,+})} \right] , \quad (43)$$

where $S^{\mathbb{C}/\mathbb{Z}_2}$ is given by eq. (11). To obtain a similarly universal answer for S_{R_1} , we also take

²²In terms of the cross-ratio (12), this corresponds to taking $\eta(w(z_{e,+}), \bar{w}(\bar{z}_{e,+}); w(z_{3,+}), \bar{w}(\bar{z}_{3,+})) \rightarrow 0$ and $\eta(w(z_{1,+}), \bar{w}(\bar{z}_{1,+}); w(z_{3,+}), \bar{w}(\bar{z}_{3,+})) \rightarrow 0$. This boundary limit is the opposite of the OPE limit described in footnote 17.

$(z_{1,+}, \bar{z}_{1,+}) \rightarrow (-\infty, 0)$ to the past boundary of the left inner horizon, in which case

$$S_{R_1} \sim S^{\mathbb{C}/\mathbb{Z}_2}(w(z_{1,+}), \bar{w}(\bar{z}_{1,+})) + S^{\mathbb{C}/\mathbb{Z}_2}(w(z_{e,+}), \bar{w}(\bar{z}_{e,+})) - \frac{c}{6} \log \left[\Omega(z_{1,+}, \bar{z}_{1,+}) \Omega(z_{e,+}, \bar{z}_{e,+}) \sqrt{w'(z_{1,+}) \bar{w}'(\bar{z}_{1,+}) w'(z_{e,+}) \bar{w}'(\bar{z}_{e,+})} \right]. \quad (44)$$

We will now explicitly evaluate the stress tensor near the inner horizon and the mutual information $I_{R_1:R_3}$ in each of the conformal vacua introduced in appendix A.2.2. The presentation will be in the reverse order in which the states were introduced, to make it clear that the entanglement near the inner horizon of an asymptotically AdS black hole is an outlier case, as expected from the arguments of section 6.

Unruh state with no infalling radiation. In the Unruh state with no infalling radiation, the stress tensor is given by eq. (38), where the Weyl factor is given by eq. (32). More precisely, eq. (38) gives the $\langle T_{\bar{z}_t \bar{z}_t} \rangle$ component of the stress tensor. Performing a coordinate transformation (not a conformal transformation, which also rescales the metric tensor) to (z_-, \bar{z}_-) and expanding near the inner horizon, we find²³

$$\langle T_{\bar{z}_- \bar{z}_-} \rangle = -\frac{c}{48\pi \bar{z}_-^2} [1 + \mathcal{O}((z_- \bar{z}_-)^2)]. \quad (45)$$

Combining eqs. (39) to (41) with eq. (2), we find the mutual information

$$I_{R_1:R_3} = \frac{c}{6} \log \left[\frac{z_{e,+} (z_{1,+} - z_{e,+}) (\bar{z}_{1,t} - \bar{z}_{e,t})}{z_{1,+} \Omega_{+t}^2(z_e, \bar{z}_e)} \right], \quad (46)$$

where Ω_{+t} is given by eq. (32) and we have sent the right endpoint of R_3 to the past boundary of the right inner horizon $(z_{3,+}, \bar{z}_{3,t}) \rightarrow (0, +\infty)$, as indicated in figure fig. 5a. Rewriting in terms of inner Kruskal coordinates and pushing the entangling surface (z_e, \bar{z}_e) towards the right inner horizon by taking small $-\bar{z}_{e,-}$, we find

$$I_{R_1:R_3} = \frac{c}{6} \log \left[\bar{z}_{e,-} \log \left(\frac{\bar{z}_{e,-}}{\bar{z}_{1,-}} \right) \right] + (\text{constant in } \bar{z}_e) + \mathcal{O}(z_{e,-} \bar{z}_{e,-}). \quad (47)$$

From eqs. (45) and (47), we see that the stress tensor has a negative quadratic divergence while the mutual information has a negative logarithmic divergence in the limit $\bar{z}_{e,-} \rightarrow 0^-$ where the inner horizon is approached from below. As a sanity check, let us consider the QNEC. Near the inner horizon, the Kruskal coordinate $\bar{z}_- \sim \lambda$ serves approximately, at leading order, as an affine parameter on the blue null line along which the black entangling surface is pushed in fig. 5a. Thus, the QNEC states

$$\langle T_{\bar{z}_- \bar{z}_-}(z_e, \bar{z}_e) \rangle \sim \langle T_{kk}(z_e, \bar{z}_e) \rangle \geq \frac{1}{4\pi} \partial_\lambda^2 I_{R_1:R_3} \sim \frac{1}{4\pi} \partial_{z_{e,-}}^2 I_{R_1:R_3} \quad (48)$$

²³Somewhat surprisingly, we have $\mathcal{O}((z_- \bar{z}_-)^2)$ instead of $\mathcal{O}(z_- \bar{z}_-)$ for the relative size of the correction in eq. (45). The assumed expansion (22) of f noted in footnote footnote 18 results in an exact cancellation of the naive next-to-leading correction in eq. (45) and also eqs. (49) and (52) further below. Note also that eq. (38) describes only conformal *vacua*.

where $k = \partial_\lambda \sim \partial_{\bar{z}_-}$. The leading divergences of eqs. (45) and (47) are certainly consistent with the QNEC.

By explicit calculation, we have shown that $I_{R_1:R_3}$ diverges negatively in the limit $\bar{z}_{e,-} \rightarrow 0^-$ where R_3 coincides with a past portion the Cauchy, inner horizon, as predicted in section 6. As explained there, the mutual information $I_{R_1:R_2}$ between the grey and yellow subregions in fig. 2a should also be negatively divergent across the Cauchy horizon. By our argument in section 5, SCC should therefore be upheld (had we been considering a gravitational theory).

Indeed, we see that the stress tensor (45) features a non-integrable divergence as the Cauchy horizon is approached — this is the signature of SCC that more standard approaches (such as [10]) usually look for. However, it should be noted that this is not the infinite *positive* energy promised by our analysis in sections 4 and 5 as a consequence of disentanglement. As already seen in the example considered in appendix A.1, the infinite positive energy which violates statement (iii) appears on (or immediately after) the surface — here, the Cauchy horizon — where the disentanglement criterion (i) is satisfied, not on approach to it. This infinite positive energy will only become apparent when one attempts any (sensible, in the sense of statement (ii)) extension of the state beyond the Cauchy horizon.

Nonetheless, we see that the QNEC (48) tells us that whenever one finds negative, non-integrably divergent null energy on approach to the Cauchy horizon, our disentanglement criterion (i) and thus our SCC argument in section 5 should also apply. Below, we will also see cases where the Cauchy horizon satisfies our disentanglement criteria (i) and (i') even when the stress tensor diverges positively or not at all as the Cauchy horizon is approached from below.

Unruh state with infalling cosmological radiation. Next, let us consider the Unruh state with infalling radiation at temperature $\kappa_c/2\pi$. In this case, the stress tensor $\langle T_{\bar{z}_c \bar{z}_c} \rangle$ is given by eq. (38) with the Weyl factor (33). Written using inner horizon Kruskal coordinates, we have

$$\langle T_{\bar{z}_- \bar{z}_-} \rangle = \frac{c}{48\pi} \frac{\kappa_c^2 - \kappa_-^2}{\kappa_-^2} \frac{1}{\bar{z}_-^2} [1 + \mathcal{O}((z_- \bar{z}_-)^2)], \quad (49)$$

in agreement with the result of [10]. The mutual information between regions R_1 and R_3 is again obtained by combining eqs. (39) to (41). Placing the right endpoint $(z_{3,+}, \bar{z}_{3,c}) \rightarrow (0, 0)$ of R_3 on the past boundary the right inner horizon, the mutual information reads

$$I_{R_1:R_3} = \frac{c}{6} \log \left[\frac{z_{e,+} \bar{z}_{e,c} (z_{1,+} - z_{e,+}) (\bar{z}_{1,c} - \bar{z}_{e,c})}{z_{1,+} \bar{z}_{1,c} \Omega_{+c}^2(z_e, \bar{z}_e)} \right] \quad (50)$$

$$= \frac{c}{6} \log \{ (-\bar{z}_{e,-}) [(-\bar{z}_{1,-})^{\kappa_c/\kappa_-} - (-\bar{z}_{e,-})^{\kappa_c/\kappa_-}] \} + (\text{constant in } \bar{z}_e) + \mathcal{O}(z_{e,-} \bar{z}_{e,-}). \quad (51)$$

In the last line, we have isolated the dependence on the small separation $-\bar{z}_{e,-}$ between the inner horizon and the entangling surface. Again, the QNEC (48) is satisfied by the leading divergences of eqs. (49) and (51).

Equation (49) describes the competition between the negative null energy background (45) previously seen in the absence of infalling radiation, and the positive null energy of

infalling cosmological radiation. Depending on the temperatures of the inner horizon and the cosmological radiation, the stress tensor can diverge positively, negatively, or not at all as one approaches the inner horizon $\bar{z}_- \rightarrow 0^-$.

In contrast, as $\bar{z}_{e,-} \rightarrow 0^-$, the negative divergence of the mutual information (51) is insensitive to these temperatures. As explained in section 6, the dS²⁴ cosmological radiation falling into the black hole is entangled with partners across the cosmological horizon that are captured by the dS future infinity \mathcal{I}^+ . Such radiation does not therefore contribute to $I_{R_1:R_3}$ significantly to alter its divergent behaviour as R_3 approaches a past portion of the inner, Cauchy horizon. Our argument for SCC in sections 5 and 6 based on this negative divergence in mutual information therefore always applies, even when more standard stress-tensor-based approaches would see no divergence at $\kappa_c = \kappa_-$.

Hartle-Hawking state. Finally, we consider the Hartle-Hawking state. Here, eq. (38) gives $\langle T_{\bar{z}_+\bar{z}_+} \rangle$ in terms of the Weyl factor (34). In inner Kruskal coordinates, this becomes

$$\langle T_{\bar{z}_-\bar{z}_-} \rangle = \frac{c}{48\pi} \frac{\kappa_+^2 - \kappa_-^2}{\kappa_-^2} \frac{1}{\bar{z}_-^2} [1 + \mathcal{O}((z_- \bar{z}_-)^2)]. \quad (52)$$

It has an interpretation similar to eq. (49); in lieu of cosmological radiation, the black hole now absorbs radiation at the outer horizon temperature $\kappa_+/2\pi$. The Hartle-Hawking state is equally applicable to asymptotically flat and AdS black holes, which both share the above near-inner-horizon behaviour of the stress tensor.²⁵

There is a drastic difference between the two cases, however, in the mutual information $I_{R_1:R_3}$. Let us consider asymptotically flat black holes first. Equations (39) to (41) are applicable in this case. Combining these into a mutual information (2) and, as always, placing the right endpoint $(z_{3,+}, \bar{z}_{3,+}) \rightarrow (0, +\infty)$ of R_3 on the past boundary of the right inner horizon, we obtain

$$\begin{aligned} I_{R_1:R_3} &= \frac{c}{6} \log \left[\frac{z_{e,+} (z_{1,+} - z_{e,+}) (\bar{z}_{1,+} - \bar{z}_{e,+})}{z_{1,+} \Omega_{++}^2(z_e, \bar{z}_e)} \right] \quad (53) \\ &= \frac{c}{6} \log \{ (-\bar{z}_{e,-}) [(-\bar{z}_{1,-})^{\kappa_+/\kappa_-} - (-\bar{z}_{e,-})^{\kappa_+/\kappa_-}] \} + (\text{constant in } \bar{z}_e) + \mathcal{O}(z_{e,-} \bar{z}_{e,-}). \quad (54) \end{aligned}$$

The behaviour (54), as the entangling surface $\bar{z}_{e,-} \rightarrow 0^-$ is pushed towards the inner horizon, is similar to eq. (51). Again, the only difference is that the temperature of the infalling radiation has been changed from $\kappa_c/2\pi$ to $\kappa_+/2\pi$. Because the Hartle-Hawking state is a thermofield double, the radiation falling in from the right exterior, in particular the r_1

²⁴As previously described, we can also consider this same conformal vacuum on asymptotically flat backgrounds, with infalling ‘‘cosmological’’ radiation at temperature $\kappa_c/2\pi$ not necessarily dictated by geometry. This is the same as the Hartle-Hawking state when $\kappa_c = \kappa_+$. Otherwise, the state is singular on the $\bar{z}_+ = 0$ piece of the outer horizon. Regardless, the interpretation of the negative divergence of mutual information is the same as described for the Hartle-Hawking state below.

²⁵In principle, one can technically consider asymptotically dS black holes in the Hartle-Hawking state, subject to the caveats described below eq. (37). Proceeding anyway, eqs. (52) to (54) would be applicable in this case.

discussed in section 6, is entangled primarily with outgoing radiation in the left exterior captured by \mathcal{S}^+ . Consequently, this radiation, much like dS cosmological radiation, does not alter the divergent behaviour of the above mutual information in the $\bar{z}_{e,-} \rightarrow 0^-$ limit.

The AdS asymptotic boundary \mathcal{S} , however, reflects outgoing radiation back into the black hole. Consequently, we concluded in section 6 that $I_{R_1:R_3}$ need not be negatively divergent in the limit $\bar{z}_{e,-} \rightarrow 0^-$ where R_3 coincides with a past portion of the inner, Cauchy horizon. Let us now see this explicitly from the entropy formulas (42) to (44) derived in the presence of the boundary. These combine to give the mutual information

$$I_{R_1:R_3} = 2S^{\mathbb{C}/\mathbb{Z}_2}(w(z_{e,+}), \bar{w}(\bar{z}_{e,+})) - \frac{c}{3} \log \left[\Omega(z_{e,+}, \bar{z}_{e,+}) \sqrt{w'(z_{e,+}) \bar{w}'(\bar{z}_{e,+})} \right] \quad (55)$$

$$= \frac{c}{6} \log \left\{ - \frac{(-\bar{z}_{e,-})^{1+\frac{\kappa_+}{\kappa_-}} [w(z_{e,+}) - \bar{w}(\bar{z}_{e,+})]^2}{\bar{w}'(\bar{z}_{e,+})} \right\} + (\text{constant in } \bar{z}_e) + \mathcal{O}(z_{e,-}, \bar{z}_{e,-}). \quad (56)$$

In eq. (55), the left endpoint of R_1 and the right endpoint of R_3 have been placed respectively at the past boundaries of the left and right inner horizons.²⁶ In fact, this can be viewed as removing the left endpoint of R_1 and the right endpoint of R_3 so that R_1 and R_3 become complementary to each other. Thus, the above is equal to double the entropy of R_1 with no left endpoint or double the entropy of R_3 , with no right endpoint.

For small $\bar{z}_{e,-}$, note that

$$\bar{w}(\bar{z}_{e,+}) = i + \frac{2R_{\mathcal{S}}}{\bar{z}_{e,+}} + \mathcal{O}(\bar{z}_{e,+}^{-2}) = i + 2R_{\mathcal{S}}(-\bar{z}_{e,-})^{\kappa_+/\kappa_-} + \mathcal{O}((-\bar{z}_{e,-})^{2\kappa_+/\kappa_-}), \quad (57)$$

so the $[w(z_{e,+}) - \bar{w}(\bar{z}_{e,+})]^2$ factor in the logarithm of eq. (56) is innocuous. It is the $(-\bar{z}_{e,-})^{1+\frac{\kappa_+}{\kappa_-}}$ factor together with

$$\bar{w}'(\bar{z}_{e,+}) = -\frac{2R_{\mathcal{S}}}{\bar{z}_{e,+}^2} + \mathcal{O}(\bar{z}_{e,+}^{-3}) = -2R_{\mathcal{S}}(-\bar{z}_{e,-})^{2\kappa_+/\kappa_-} + \mathcal{O}((-\bar{z}_{e,-})^{3\kappa_+/\kappa_-}) \quad (58)$$

which determines the divergent behaviour of eq. (56) as $\bar{z}_{e,-} \rightarrow 0^-$. These factors originate from the second term in eq. (55) describing the conformal and Weyl transformation

²⁶Notice here that, relative to cases we previously considered, we have fixed an extra freedom by pushing the left endpoint of R_1 to the past boundary of the left inner horizon. As explained above eq. (44) and in footnote 22, we did this to evaluate a two-point function in the half-plane by taking an extreme limit $\eta(w(z_{1,+}), \bar{w}(\bar{z}_{1,+}); w(z_{e,+}), \bar{w}(\bar{z}_{e,+})) \rightarrow 0$ of the cross-ratio defined in eq. (12).

One might wonder if this is the underlying reason why the $\bar{z}_{e,-} \rightarrow 0^-$ divergence we are finding for $I_{R_1:R_3}$ in AdS is so different from previously considered cases — let us dissuade against this thinking. Suppose that η had not been taken to an extreme value, 0 or ∞ , by our choice of the left endpoint of R_1 . Then the first line of eq. (44) would generally be replaced by something with also nontrivial dependence on η , not fixed by conformal invariance. However, just as a half-plane two-point function should be finite except when the insertions collide with each other or with the boundary, the corrected first line of eq. (44) should remain finite apart from $\eta \rightarrow 0, \infty$. Taking $\bar{z}_{e,-} \rightarrow 0^-$ at fixed $z_{e,+} < 0$ does not send $\eta \rightarrow 0, \infty$ unless η was already at these extreme values to begin with. Thus, whatever nontrivial η -dependence acquired by the corrected first line of eq. (44) cannot contribute to divergences in $I_{R_1:R_3}$ as $\bar{z}_{e,-} \rightarrow 0^-$. The only possible divergences are from the second, transformation term in eq. (55), just as we find below.

between the w half-plane and the black hole geometry. We see that the leading divergence $\frac{c}{6} \frac{\kappa_+ - \kappa_-}{\kappa_-} \log(-1/\bar{z}_{e,-})$ of eq. (56) is consistent with the QNEC (48) and the stress tensor (52).

This divergence in mutual information can be negative, zero, or positive, depending on whether the outer horizon temperature $\kappa_+/2\pi$ is less than, equal to, or greater than the inner horizon temperature $\kappa_-/2\pi$, in contrast to all cases we have considered previously. Of course, this is consistent with our discussion in section 6, where we explained how Cauchy horizons in AdS black holes may present outlying exceptions to our disentanglement criteria. From our disentanglement argument alone, it may therefore appear that mutual information is a weaker probe of SCC in AdS than the stress tensor, which diverges except when $\kappa_+ = \kappa_-$. However, let us point out that positive divergences of mutual information are also dangerous: instead of applying our disentanglement argument, one can appeal directly to the QNEC (48), which states *e.g.* that a positive logarithmic divergence in mutual information (or entropy) leads to a positive quadratic divergence in the stress tensor. The QFC (6) is similarly helpful, with dynamical gravity.²⁷

References

- [1] M. Van Raamsdonk, *Building up spacetime with quantum entanglement*, *Gen. Rel. Grav.* **42** (2010) 2323 [1005.3035].
- [2] J. Maldacena and L. Susskind, *Cool horizons for entangled black holes*, *Fortsch. Phys.* **61** (2013) 781 [1306.0533].
- [3] A. Almheiri, N. Engelhardt, D. Marolf and H. Maxfield, *The entropy of bulk quantum fields and the entanglement wedge of an evaporating black hole*, *JHEP* **12** (2019) 063 [1905.08762].
- [4] G. Penington, *Entanglement Wedge Reconstruction and the Information Paradox*, *JHEP* **09** (2020) 002 [1905.08255].
- [5] S.W. Hawking, *Breakdown of Predictability in Gravitational Collapse*, *Phys. Rev. D* **14** (1976) 2460.
- [6] A. Almheiri, D. Marolf, J. Polchinski and J. Sully, *Black Holes: Complementarity or Firewalls?*, *JHEP* **02** (2013) 062 [1207.3123].
- [7] B. Czech, J.L. Karczmarek, F. Nogueira and M. Van Raamsdonk, *Rindler Quantum Gravity*, *Class. Quant. Grav.* **29** (2012) 235025 [1206.1323].
- [8] R. Bousso, Z. Fisher, S. Leichenauer and A.C. Wall, *Quantum focusing conjecture*, *Phys. Rev. D* **93** (2016) 064044 [1506.02669].
- [9] R. Penrose, *Gravitational collapse, Symposium - International Astronomical Union* **64** (1974) 82–91.

²⁷Considering I_{R_1, R_3} , one might worry about the validity of the QFC due to the large extrinsic curvature [39] present in the slice containing $R_1 \cup R_3$ as the entangling surface is pushed to the Cauchy, inner horizon. But, as mentioned below eq. (56), for AdS, it suffices to work with just the entropy of R_1 .

- [10] S. Hollands, R.M. Wald and J. Zahn, *Quantum instability of the Cauchy horizon in Reissner–Nordström–deSitter spacetime*, *Class. Quant. Grav.* **37** (2020) 115009 [1912.06047].
- [11] K. Papadodimas, S. Raju and P. Shrivastava, *A simple quantum test for smooth horizons*, *JHEP* **12** (2020) 003 [1910.02992].
- [12] W.G. Unruh, *Notes on black hole evaporation*, *Phys. Rev. D* **14** (1976) 870.
- [13] L. Susskind and J. Uglum, *Black hole entropy in canonical quantum gravity and superstring theory*, *Phys. Rev. D* **50** (1994) 2700 [hep-th/9401070].
- [14] R. Bousso, Z. Fisher, J. Koeller, S. Leichenauer and A.C. Wall, *Proof of the Quantum Null Energy Condition*, *Phys. Rev. D* **93** (2016) 024017 [1509.02542].
- [15] R. Bousso, *A Covariant entropy conjecture*, *JHEP* **07** (1999) 004 [hep-th/9905177].
- [16] R. Bousso and N. Engelhardt, *Generalized Second Law for Cosmology*, *Phys. Rev. D* **93** (2016) 024025 [1510.02099].
- [17] A. Almheiri, R. Mahajan and J. Maldacena, *Islands outside the horizon*, 1910.11077.
- [18] T. Hartman, Y. Jiang and E. Shaghoulian, *Islands in cosmology*, *JHEP* **11** (2020) 111 [2008.01022].
- [19] C. Akers, J. Koeller, S. Leichenauer and A. Levine, *Geometric Constraints from Subregion Duality Beyond the Classical Regime*, 1610.08968.
- [20] C. Akers, V. Chandrasekaran, S. Leichenauer, A. Levine and A. Shahbazi Moghaddam, *Quantum null energy condition, entanglement wedge nesting, and quantum focusing*, *Phys. Rev. D* **101** (2020) 025011 [1706.04183].
- [21] A.C. Wall, *Testing the Generalized Second Law in 1+1 dimensional Conformal Vacua: An Argument for the Causal Horizon*, *Phys. Rev. D* **85** (2012) 024015 [1105.3520].
- [22] S. Balakrishnan, T. Faulkner, Z.U. Khandker and H. Wang, *A General Proof of the Quantum Null Energy Condition*, *JHEP* **09** (2019) 020 [1706.09432].
- [23] R. Parentani, *The Energy momentum tensor in Fulling-Rindler vacuum*, *Class. Quant. Grav.* **10** (1993) 1409 [hep-th/9303062].
- [24] P. Calabrese and J. Cardy, *Entanglement and correlation functions following a local quench: a conformal field theory approach*, *J. Stat. Mech.* **0710** (2007) P10004 [0708.3750].
- [25] T. Ugajin, *Two dimensional quantum quenches and holography*, 1311.2562.
- [26] T. Shimaji, T. Takayanagi and Z. Wei, *Holographic Quantum Circuits from Splitting/Joining Local Quenches*, *JHEP* **03** (2019) 165 [1812.01176].

- [27] A. Anderson and B.S. DeWitt, *Does the Topology of Space Fluctuate?*, *Found. Phys.* **16** (1986) 91.
- [28] R. Penrose, *Structure of space-time*, in *Battelle Rencontres*, pp. 121–235, 1968.
- [29] P. Hintz and A. Vasy, *Analysis of linear waves near the Cauchy horizon of cosmological black holes*, *J. Math. Phys.* **58** (2017) 081509 [1512.08004].
- [30] V. Cardoso, J.a.L. Costa, K. Destounis, P. Hintz and A. Jansen, *Quasinormal modes and Strong Cosmic Censorship*, *Phys. Rev. Lett.* **120** (2018) 031103 [1711.10502].
- [31] O.J.C. Dias, H.S. Reall and J.E. Santos, *The BTZ black hole violates strong cosmic censorship*, *JHEP* **12** (2019) 097 [1906.08265].
- [32] V. Balasubramanian, A. Kar and G. Sárosi, *Holographic Probes of Inner Horizons*, *JHEP* **06** (2020) 054 [1911.12413].
- [33] R. Emparan and M. Tomašević, *Strong cosmic censorship in the BTZ black hole*, *JHEP* **06** (2020) 038 [2002.02083].
- [34] M. Kolanowski and M. Tomašević, *Singularities in 2D and 3D quantum black holes*, *JHEP* **12** (2023) 102 [2310.06014].
- [35] P. Shrivastava, *Quantum aspects of charged black holes in de-Sitter space*, 2009.03261.
- [36] D. Stanford and Z. Yang, *Firewalls from wormholes*, 2208.01625.
- [37] I. Affleck and A.W.W. Ludwig, *Universal noninteger 'ground state degeneracy' in critical quantum systems*, *Phys. Rev. Lett.* **67** (1991) 161.
- [38] N.D. Birrell and P.C.W. Davies, *Quantum Fields in Curved Space*, Cambridge Monographs on Mathematical Physics, Cambridge Univ. Press, Cambridge, UK (2, 1984), 10.1017/CBO9780511622632.
- [39] R. Bousso and A. Shahbazi-Moghaddam, *Quantum singularities*, *Phys. Rev. D* **107** (2023) 066002 [2206.07001].